Phase-Matched Generation of Coherent Soft X-rays

Andy Rundquist, *et al.*
Science **280**, 1412 (1998);
DOI: 10.1126/science.280.5368.1412

Phase-Matched Generation of Coherent Soft X-rays

Andy Rundquist, Charles G. Durfee III, Zenghu Chang, Catherine Herne, Sterling Backus, Margaret M. Murnane,* Henry C. Kapteyn

Phase-matched harmonic conversion of visible laser light into soft x-rays was demonstrated. The recently developed technique of guided-wave frequency conversion was used to upshift light from 800 nanometers to the range from 17 to 32 nanometers. This process increased the coherent x-ray output by factors of 10^2 to 10^3 compared to the non–phase-matched case. This source uses a small-scale (sub-millijoule) high repetition-rate laser and will enable a wide variety of new experimental investigations in linear and nonlinear x-ray science.

Nonlinear optical techniques for frequency conversion have played a pivotal role in the development of efficient coherent light sources (1), second in significance only to the invention of the laser itself. In recent years, nonlinear optics has led to the development of efficient visible-wavelength laser sources and sources with broad tunability such as optical parametric oscillators (2) and amplifiers (3). Most recently, the use of structured materials has made possible a new class of efficient nonlinear optical devices based on quasi–phase-matching (4).

However, nonlinear frequency-conversion techniques have almost exclusively relied on crystalline solids as nonlinear media. For efficient conversion, the electromagnetic waves corresponding to the driving and the generated signal must be phase-matched—both colors of light must have the same phase velocity as they travel through the generating medium. In this case, the nonlinear polarization adds coherently as the waves co-propagate, resulting in a rapid increase in signal intensity. To date, phase-matching has generally been achieved by relying on a combination of anisotropic materials and differing source and signal polarizations, because unless conditions are chosen carefully, light of different colors travel at different speeds through a material.

This reliance on solid materials has severely limited the application of nonlinear optical techniques to very short wavelengths. The best solid nonlinear materials such as lanthanum boron oxide (LBO) and barium boron oxide (BBO) can be used to generate light at wavelengths as short as 200 nm (5). However, few solids are transparent at wavelengths shorter than this, and
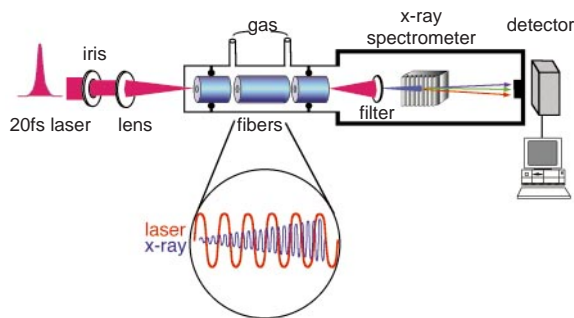
none are transparent in the extreme ultraviolet (XUV) and soft x-ray regions of the spectrum. In contrast, many gases are transparent well into the vacuum ultraviolet (VUV), and even shorter wavelengths can propagate with moderate absorption through low-pressure gases. However, because gases are isotropic, established phase-matching techniques are not applicable, and thus, phase-matched frequency conversion techniques have not been developed for the XUV and soft x-ray regions of the spectrum.

Nevertheless, in recent years the technique of high-harmonic generation (HHG) has proven to be a useful source of XUV and soft x-ray light (6, 7). In this process, atoms in a dilute gas radiate harmonics of the incident light in the process of being ionized at the focus of an intense ultrashort-pulse laser. The highly nonlinear nature of the ionization process makes it possible to generate harmonics up to order 299 and higher at wavelengths below 3 nm, using very short laser pulses (8, 9). Despite the low efficiency of this process ($<10^{-8}$ conversion of laser light into one harmonic peak), the photon flux generated is still sufficient to be useful for some applications in ultrafast x-ray spectroscopy. The HHG technique is also of considerable theoretical interest as a possible method for generating attosecond-duration light pulses (10–12).

However, many more applications would be possible if the process were made more efficient by phase-matching. Unfortunately, the rapidly changing free-electron density associated with ionization of the atoms led to the generally held opinion that phase-matching would result in, at most, modest improvements in efficiency (13–15), because the length over which the harmonic phase slips by π from the laser (the coherence length) is ≈ 50 μm for a fully ionized gas. Phase-matching would compensate for this phase slippage (Fig. 1, inset) and allow the x-ray emission from much longer lengths to add coherently.

We report a phase-matching technique that circumvents the limitations of crystalline nonlinear optics by making phase-matched frequency conversion of ultrashort-pulse laser light into the XUV possible. Phase-matched frequency conversion in gases has been achieved in the UV spectrum in past experiments by exploiting the negative dispersion that exists for light at wavelengths just shorter than a resonant absorption line (16, 17). However, the resonant requirement limits the phase-matching bandwidth, making it difficult to use this technique for applications that require broad tunability or ultrashort pulses, and also limits the conversion efficiency. Moreover, most experiments in HHG to date have been done in the tight focusing geometry, where the phase shift due to the laser focus dominates and limits phase-matching (18). Although proper choice of focusing conditions can somewhat increase the coherence length, the useful interaction length is still fundamentally limited by the laser beam divergence. In contrast, by propagating a light pulse through a wave guide, its phase velocity can be carefully controlled and the beam divergence effects eliminated. Previous work has proposed the use of a transient wave guide created by a laser-produced plasma for phase-matched frequency conversion using high-order frequency mixing (19). However, as we show, a hollow capillary tube allows phase-matching in neutral gas with single frequency input, while employing a much simpler experimental configuration. The phase veloc-

Center for Ultrafast Optical Science, University of Michigan, Ann Arbor, MI 48109–2099, USA.

*To whom correspondence should be addressed. E-mail: murnane@umich.edu

Fig. 1. Experimental set-up for phase-matching of soft x-rays in a capillary wave guide. The inset shows the growth of the x-ray wave when phase-matched. Note that the laser and x-ray wavelengths are not to scale.

ity of the laser light in a hollow wave guide can be adjusted by simply changing the guide diameter or by changing the gas pressure inside the wave guide. Thus, very long coherence and interaction lengths can be obtained, with a corresponding increase in conversion efficiency.

Using the guided-wave frequency conversion technique of phase-matching and a four-wave mixing scheme (20), we previously demonstrated very high (20%) conversion efficiency of ultrashort light pulses into the UV region. This finding immediately led to the question of whether guided-wave phase-matching could be applied to the x-rays generated as high-harmonic radiation. If HHG is directly and inextricably linked to ionization, one must contend with the effects of a rapidly varying index of refraction. Furthermore, the intensities used for HHG might cause damage to the wave guide structure. Even if the light does not cause damage, the reactive ionized gas might. We show that it is indeed possible to generate efficient high-harmonic XUV radiation in a fiber, in a regime where ionization-induced index of refraction effects are minimized. We achieve this by using short (20 fs) pulses to create the x-ray harmonics. A shorter pulse reduces the level of ionization at which a particular pulse intensity is reached, making it possible to generate high harmonics in a regime where the ionization-induced index does not preclude phase-matching. Experimentally, we have generated >0.2 nJ of x-rays per harmonic per pulse at a 1-kHz repetition-rate, with pulse durations expected to be under 5 fs, in a near-diffraction-limited beam. Using this source, it should be possible to produce focused x-ray intensities of $>10^{14}$ W cm^{-2}, assuming f/10 focusing. Straightforward improvements to our scheme should lead to further enhancements in x-ray output by at least an order of magnitude. Therefore, using higher repetition rate (10 kHz) millijoule-level lasers, it should be possible to generate fractions of a milliwatt power per harmonic peak. Even the current several microwatts of power over 10 harmonic orders compares favorably with the average power produced by the current generation of soft x-ray lasers. The development of our source will thus make possible new types of investigations in linear and nonlinear x-ray science and technology.

Guided-wave frequency conversion is possible because of the frequency-dependent dispersion introduced by light propagation in a wave guide. By confining the beam, a wave guide structure gives an additional, geometric component to the phase velocity (21). In a ray picture, the inside walls of the hollow wave guide confine the beam by repeated glancing-incidence re-

flections. The intrinsic diffraction, and thus the effective grazing angle of incidence on the walls, increases with wavelength. Because the projection of the wave vector along the optical axis is shorter than in free space, the phase velocity of the guided beam increases with wavelength. From another perspective, the discrete modes of the wave guide are standing waves in the transverse direction. When the wave guide k-vector corresponding to the wavelength of this standing wave is added to the free-space wave vector, diffraction is canceled. Because the wave guide k-vector is frequency independent whereas the free-space propagation k-vector is longer for shorter wavelength, the net k-vector is most strongly perturbed for long-wavelength light. Mathematically, for light traveling in the wave guide, the k-vector of propagation is

$$k \approx \frac{2\pi}{\lambda} + \frac{2\pi N_a\,\delta(\lambda)}{\lambda} - N_e r_e \lambda - \frac{u_{nm}^2 \lambda}{4\pi a^2}$$

where the first term corresponds to simple vacuum propagation, and the second and third result from dispersion of the gas and of the plasma, respectively, created by ionization. Here, N_a is the atom density, N_e is the electron density, and δ depends on the dispersive characteristics of the atom. The last term corresponds to the wave guide, where a is the radius of the wave guide and u_{nm} is a constant corresponding to the propagation mode in the fiber. The net phase mismatch for a nonlinear mixing process results from the vector sum of all of the waves involved, with source waves added and signal wave subtracted. Phase-matching corresponds to $\Delta k = q k_{laser} - k_{x-ray} = 0$, where q is the harmonic order. The gas-filled hollow wave guide allows many adjustment parameters by which the phase-matched condition can be engineered: the wavelength, gas pressure, gas species, wave guide size, and the spatial mode.

The case of HHG is particularly simple. The interactions of the soft x-ray light with the wave guide is minimal, and the phase velocity of the x-rays is thus slightly greater than c (the speed of light in vacuum). The phase velocity of the laser is the balance of three competing terms: the wave guide dispersion and plasma dispersion, which increase the phase velocity, and the material dispersion, which decreases it. Because these contributions are of opposite sign, by varying the pressure of the gas, we can achieve the phase-matched condition where the x-ray and laser light travel with the same speed. This is shown conceptually in the inset to Fig. 1. The presence of ionization-induced plasma changes the dispersion substantially. However, by varying the gas pressure, phase-matching can be

regained as long as the total percentage of ionized atoms is still small ($<\sim$5% for argon). The use of 20-fs pulses allows us to keep the total ionization fraction small but still achieve intensities that are sufficient for generating XUV harmonics of up to the 45th order.

A schematic of our experiment is shown in Fig. 1. We used a titanium-doped sapphire laser amplifier system, with a wavelength of 800 nm (1.55 eV photon energy) (22). Pulses from a Kerr-lens mode-locked oscillator (23) were amplified at a repetition rate of 1 kHz in two multipass laser amplifier stages capable of generating 4.5 mJ in a 17-fs pulse duration. For these experiments, pulses of energy 100 to 300 μJ, with a pulse duration of 20 fs, were directed through an iris and focused with a 300-mm focal length fused silica lens through a sapphire chamber entrance window into a differentially pumped capillary cell. The laser waist size is 50 μm in the fiber. The capillary cell is a three-segment design that allows a relatively high, and more important, constant gas pressure within the capillary while greatly restricting the flow of gas into the vacuum regions at either end. If a prefiber was not used, the presence of gas before the first fiber could lead to ionization-induced defocusing of the laser beam. Three sections of capillary tube, with 150 μm inside diameter and 6.3 mm outside diameter, were held in a V-groove with spacing between the segments of ~1 mm. This design allowed a guided laser beam to pass from one section to another with minimal absorption loss. The total capillary length was 6.4 cm, with a central section length of 3 cm. Flexible coupling to the vacuum system on either side permitted the capillary to be aligned properly. The input iris was used to adjust the focal spot diameter to match that of the lowest-order mode of the capillary wave guide. The light emerging from the capillary was aligned through an imaging grazing incidence spectrometer (HiREFS SXR-1.75; Hettrick Scientific, Kensington, CA). A thin aluminum filter (0.2 μm) was used to block the laser light and pass only the 11th through 45th harmonics (17 to 70 eV). The signal was detected with a microchannel plate coupled to a phosphor screen (XSI, Ann Arbor, MI). The image was either viewed with a charge-coupled device camera or integrated with a photodetector. Laser damage to the capillary fiber was not a problem; although misalignment at high power can cause damage, with proper alignment and at the intensities used for these experiments, no degradation of the capillary wave guide was observed after tens of hours of operation at a 1-kHz repetition-rate. The pumping speed required to maintain good vacuum in the spectrometer is also very greatly reduced compared with harmon-

ic generation in a pulsed-gas nozzle or free-flowing cell, which have been used in the past for HHG experiments.

If phase-matching of conversion of laser light into x-rays is achieved, we should observe a marked increase in x-ray output at the optimum pressure for a given harmonic order. Propagation in the wave guide is basically plane-wave, and losses of the laser over the propagation length in the fiber (a few centimeters in these experiments) are minimal. Thus, for any given position temporally within the pulse and copropagating with it, the level of ionization is constant, and an optimum pressure and intensity can be found in the constant-density middle section. Typical data for the 29th and 31st harmonic of 800 nm at 28 and 26 nm, respectively, generated in a 150-μm capillary filled with argon, are shown in Fig. 2. The theoretically predicted output is shown in Fig. 3. At pressures of 35 torr, phase-matching is predicted and observed to occur and caused a dramatic increase in harmonic

output. We checked that for pressures up to 200 torr, no change in the transmission of the laser light occurred because of ionization effects. Therefore, the decrease in signal at high pressures is due to the loss of phase-matching because of excess gas dispersion, and not due to ionization-induced defocusing. A further confirmation of this explanation is that the optimum phase-matched pressure shifts to higher pressures if the laser intensity is increased. The increased intensity adds a negative contribution to the refractive index because of increased ionization, which must be balanced by a higher gas pressure. At pressures of 30 to 50 torr, a total of five harmonic peaks (orders 23 through 31) are phase-matched. However, the optimum phase-matching pressure for each harmonic is slightly different, because the higher harmonics are generated at higher values of ionization. No signal was observed for harmonic orders below the 23rd because of strong absorption in the argon gas. This is a strong indication that the observed harmonic light is generated primarily within the central fiber segment. Also, at the peak intensities used in these experiments ($\approx 2 \times 10^{14}$ W cm^{-2}), we only expect to observe harmonics up to order 31. The higher harmonic orders (orders 33 through 45) are phase-matched by increasing the gas pressure and laser intensity.

Figure 3 shows the theoretically predicted output for the 29th harmonic, with and without the presence of absorption and ionization. The presence of absorption and ionization tends to dampen and broaden the expected oscillations of the output signal with pressure, both because the absorption depth (8 mm) is shorter than the coherence length and because the harmonics are generated over a range of ionization levels, each optimizing at a slightly different pressure. The presence of ionization ($\approx 2\%$ when the harmonic is being generated) tends to shift the optimum phase-matched pressure to higher values (Fig. 3, B and D) because of the need to balance the refractive index contribution introduced by ionization to maintain phase-matching. Absorption in the gas reduces the expected output by an order of magnitude (Fig. 3). This absorption explains why our output is enhanced only by factors of 10^2 to 10^3 (see below), instead of the maximum expected enhancements of 10^4 due to the increase in coherence length from 50 μm to an interaction length of a few centimeters. The coherence length is infinite when phase-matched.

The conversion efficiency of laser light into a single harmonic peak was measured in two independent ways. First, a vacuum photodiode (XSI) was inserted before the x-ray spectrometer, and the current was recorded with a picoammeter (Keithley 485; Keithley, Cleveland, OH). A metal filter was placed between the source and detector to block any low-order harmonics that might have been present. In practice, this procedure was not necessary, because the low-order harmonics are not phase-matched at this pressure and also are strongly absorbed in argon, and therefore, their signal levels are orders of magnitude below that of the five phase-matched harmonics. Signal levels of ~100 pA were observed. Given our repetition rate of 1 kHz, a detector quantum efficiency of at best 0.08, a measured filter transmission of 10%, and an input laser energy of 150 μJ per pulse, we estimate that $> 2 \times 10^7$ photons per harmonic peak per pulse were emitted. This value corresponds to an energy of > 0.2 nJ per harmonic peak per pulse, or a conversion efficiency of 10^{-6} to 10^{-5} into a single harmonic peak—an increase of 100 times over previously measured efficiencies (6). We also estimated the enhancement factors by comparing our output from the fiber with that from a gas jet (7). We estimate an increase in efficiency of 10^2 to 10^3 due to phase-matching. We note that the use of the vacuum photodiode x-ray detector significantly improved the accuracy of our conversion efficiency measurements, compared with
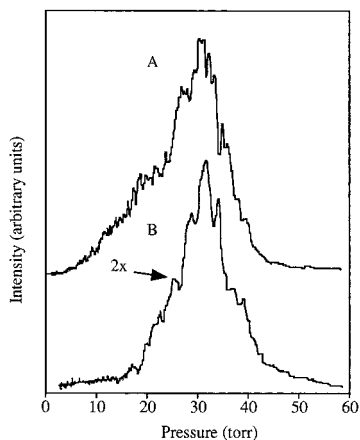

Fig. 2. Measured signals of the (**A**) 29th and (**B**) 31st harmonics as a function of gas pressure.
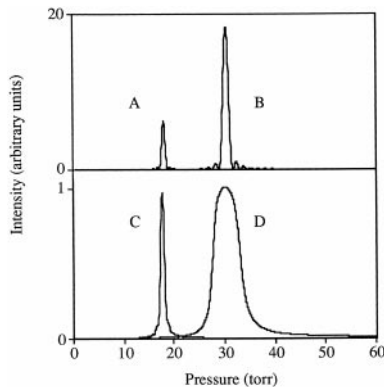

Fig. 3. (**A**) Calculated output of the 29th harmonic, (**B**) in the presence of constant 2% ionization, (**C**) in the presence of absorption, and (**D**) net output in the presence of absorption and varying levels of ionization around 2%.
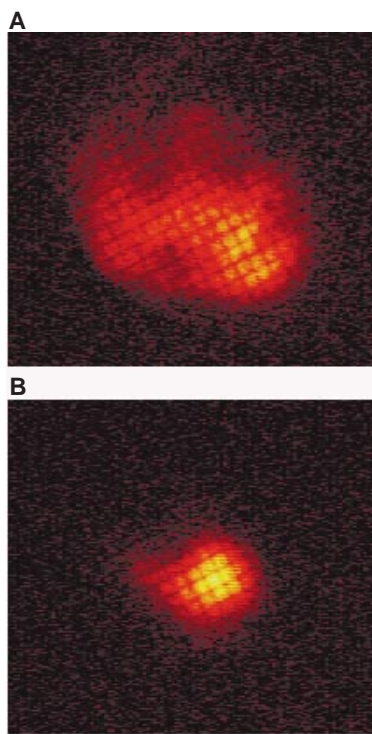

Fig. 4. Soft x-ray output beam for harmonic orders 23 through 31: (**A**) unphase-matched, detector set to high gain, and (**B**) phase-matched, detector set to low gain.

those made using other types of detectors.

An image of the phase-matched harmonic output was obtained by placing an imaging microchannel plate detector (XSI) before the spectrometer at a distance of 0.68 m from the output of the capillary. The observed harmonic beam images for harmonics 23 to 31 are shown (Fig. 4). Figure 4A shows the harmonic output beam, which is not phase-matched, at low pressures. Because in the absence of phase-matching the harmonic generation is not associated with any one particular mode of the wave guide, the beam quality is poor. In contrast, Fig. 4B shows the output harmonic beam at a pressure of 35 torr, when phase-matching is optimized. Because the fundamental wave guide mode is now phase-matched to create the x-ray output, the x-rays generated have excellent spatial properties. The grid pattern which is apparent on the image is due to the ~27 lines/cm mesh on which the x-ray filter is mounted. The x-ray beam full-width-at-half-maximum diameter is ≈ 1 mm. Given our source distance of 0.68 m and the source size of radius ≈ 20 μm, the measured diffraction angle of ~1 mrad is consistent with a near-diffraction-limited x-ray output beam.

In future experiments, more optimal laser-fiber coupling, larger diameter fibers (which reduce absorption loss), lower absorption gases, and use of shorter pulses should allow significant increases in the efficiency of the phase-matched harmonic conversion process. By using recent advances in laser technology, it should be straightforward to generate milliwatts of power per harmonic peak. It should also be possible to apply this technique to shorter wavelengths, thus enabling a wide variety of new experimental investigations in linear and nonlinear x-ray science.

REFERENCES AND NOTES

1. P. A. Franken, A. E. Hill, C. W. Peters, G. Weinreich, *Phys. Rev. Lett.* **7**, 118 (1961).
2. C. Tang, W. Bosenberg, T. Ukachi, R. Lane, L. Cheng, *Proc. IEEE* **80**, 365 (1992).
3. P. Di-Trapani *et al.*, *J. Opt. Soc. Am. B* **14**, 1245 (1997).
4. L. Myers *et al.*, *ibid.* **12**, 2102 (1995).
5. U. Heitmann, M. Kotteritzsch, S. Heitz, A. Hese, *Appl. Phys. B* **55**, 419 (1992).
6. A. L'Huillier and P. Balcou, *Phys. Rev. Lett.* **70**, 774 (1993).
7. J. Zhou, J. Peatross, M. M. Murnane, H. C. Kapteyn, I. P. Christov, *ibid.* **76**, 752 (1996).
8. Z. Chang, A. Rundquist, H. Wang, M. M. Murnane, H. C. Kapteyn, *ibid.* **79**, 2967 (1997).
9. Ch. Spielmann *et al.*, *Science* **278**, 661 (1997).
10. P. B. Corkum, N. H. Burnett, M. Y. Ivanov, *Opt. Lett.* **19**, 1870 (1994).
11. I. P. Christov, M. M. Murnane, H. C. Kapteyn, *Phys. Rev. Lett.* **78**, 1251 (1997).
12. P. Antoine *et al.*, *Phys. Rev. A* **56**, 4960 (1997).
13. C. Kan, C. Capjack, R. Rankin, T. Brabec, N. Burnett, *ibid.* **54**, R1026-0 (1996).
14. A. L'Huillier, X. Li, L. Lompre, *J. Opt. Soc. Am. B* **7**, 527 (1990).
15. S. C. Rae, K. Burnett, J. Cooper, *Phys. Rev. A* **50**, 3438 (1994).
16. A. H. Kung, J. F. Young, S. E. Harris, *Appl. Phys. Lett.* **22**, 301 (1973).
17. R. Mahon, T. J. McIlrath, V. P. Myerscough, D. W. Koopman, *IEEE J. Quantum Electron.* **QE-15**, 444 (1979).
18. A. L'Huillier, K. J. Schafer, K. C. Kulander, *Phys. Rev. Lett.* **66**, 2200 (1991).
19. H. Milchberg, C. Durfee III, T. McIlrath, *ibid.* **75**, 2494 (1995).
20. C. G. Durfee, S. Backus, M. M. Murnane, H. C. Kapteyn, *Opt. Lett.* **22**, 1565 (1997).
21. E. A. J. Marcateli and R. A. Schmeltzer, *Bell Syst. Tech. J.* **43**, 1783 (1964).
22. S. Backus, C. G. Durfee, G. A. Mourou, H. C. Kapteyn, M. M. Murnane, *Opt. Lett.* **22**, 1256 (1997).
23. M. T. Asaki *et al.*, *ibid.* **18**, 977 (1993).
24. We gratefully acknowledge support from NSF. H.C.K. acknowledges support from an Alfred P. Sloan Foundation Fellowship.

23 February 1998; accepted 13 April 1998

Electrical Conductivity of Olivine, Wadsleyite, and Ringwoodite Under Upper-Mantle Conditions

Yousheng Xu,* Brent T. Poe, Thomas J. Shankland,†
David C. Rubie

Geophysical models show that electrical conductivity in Earth's mantle rises about two orders of magnitude through the transition zone in the depth range 410 to 660 kilometers. Impedance measurements obtained on $Mg_{1.8}Fe_{0.2}SiO_4$ olivine, wadsleyite, and ringwoodite at up to 20 gigapascals and 1400°C show that the electrical conductivities of wadsleyite and ringwoodite are similar and are almost two orders of magnitude higher than that of olivine. A conductivity-depth profile to 660 kilometers, based on these laboratory data, shows a conductivity increase of almost two orders of magnitude across the 410-kilometer discontinuity; such a profile favors a two-layer model for the upper mantle. Activation enthalpies of 1.2 to 1.7 electron volts permit appreciable lateral variations of conductivity with lateral temperature variations.

Estimates of the mineralogy, composition, and temperature of Earth's mantle come mainly from comparisons of seismic velocity data with measurements of the elasticity and density of potential mantle minerals (*1*). Refinements of such estimates can be derived by comparing electrical conductivity models with laboratory measurements of the conductivity of proposed mantle minerals (*2–5*). Electrical conductivity as a function of depth is calculated by inverting geomagnetic and magnetotelluric data, but such data can be fit to a range of models in which conductivity either varies smoothly with depth or changes abruptly at certain depths. In the latter case, models have been proposed in which conductivity increases rapidly, for example, at depths of 410 km (*2*), ~500 km (*3, 4*), and ~660 km (*3, 4*).

One reason for uncertainties in the electrical conductivity of the mantle is the lack of laboratory measurements on transition-zone minerals. In the depth range 410 to 660 km, the most abundant upper-mantle mineral, $Mg_{1.8}Fe_{0.2}SiO_4$ olivine, transforms to the high-pressure polymorphs wadsleyite (~410 km depth) and ringwoodite (~520 km) and then disproportionates to (Mg,Fe)-SiO_3 perovskite + (Mg,Fe)O (~660 km). Olivine conductivity has been measured at 1 bar and at pressures to 5 GPa (*6*). Omura (*7*) measured the conductivities of wadsleyite and ringwoodite with expected mantle compositions, Fe/(Mg + Fe) ≈ 0.1. These results, which suggest that conductivity increases by a factor of ~2 at the olivine-wadsleyite transition and by ~5 for a wadsleyite-ringwoodite transition, have been debated on the basis of experimental complications (*8*).

We have measured conductivities of $Mg_{1.8}Fe_{0.2}SiO_4$ olivine, wadsleyite, and ringwoodite up to 20 GPa and 1400°C within their respective stability fields (Fig. 1) (*9, 10*). The starting material was San Carlos olivine $Mg_{1.8}Fe_{0.2}SiO_4$ to which 5 weight % $Mg_{0.915}Fe_{0.085}SiO_3$ orthopyroxene was added to buffer silica activity. The small volume fraction of pyroxene has little influence on bulk conductivity. To minimize changes in the sample geometry at high pressures and iron loss to the electrodes during extended periods at high temperatures, we synthesized the polycrystalline samples in separate hot-pressing experiments and, in the case of high-pressure phases, phase-transformation experiments (*11*).

Bayerisches Geoinstitut, Universität Bayreuth, D-95440 Bayreuth, Germany.

*To whom correspondence should be addressed. E-mail: yousheng.xu@uni-bayreuth.de
†On leave from Earth and Environmental Sciences Division, Los Alamos National Laboratory, Los Alamos, NM 87545, USA.